ELSEVIER

Journal of Non-Crystalline Solids 273 (2000) 8–18

JOURNAL OF NON-CRYSTALLINE SOLIDS

www.elsevier.com/locate/jnoncrysol

# $^{29}$Si MAS–NMR studies of $Q^n$ structural units in metasilicate glasses and their nucleating ability

J. Schneider [a], V.R. Mastelaro [a,*], H. Panepucci [a], E.D. Zanotto [b]

[a] *Instituto de Física de São Carlos, Universidade de Sao Paulo, C.P. 369, 13560-970 São Carlos, SP, Brazil*
[b] *Departamento de Engenharia de Materiais, UFSCar 13565-905, São Carlos, SP, Brazil*

**Abstract**

The purpose of this work is to verify the possible existence of a relationship between the similarity of the local structure of the network-forming cation $Si^{4+}$ ($Q^n$ units and chemical shifts) in glasses and isochemical crystals and the nucleating ability of these glasses. Four metasilicate glasses with widely different volume nucleation rates: $Na_2Ca_2Si_3O_9$ and $Na_4CaSi_3O_9$ (very large), $CaSiO_3$ (intermediate) and $CaMgSi_2O_6$ (undetectably small) were chosen. We present magic angle spinning nuclear magnetic resonance spectroscopy (MAS–NMR) data for $Na_2Ca_2Si_3O_9$ and $Na_4CaSi_3O_9$ glasses and for their respective isochemical crystalline phases for the first time. Additionally, we repeat NMR measurements of glasses and crystals previously studied by other authors ($CaSiO_3$ and $CaMgSi_2O_6$) to test the consistency of our experimental techniques and method of analysis. Different central chemical shifts of $Q^2$ resonances in parent glasses and their isochemical crystals were measured, indicating structural differences. The relative amount of $Q^n$ groups in each glass was obtained from the deconvolution of the $^{29}$Si MAS–NMR spectra. The *shape* of the $Q^n$ distribution for each system was considered as a measure of the similarity of the connectivities of $SiO_4$ tetrahedra in each glass with respect to its isochemical crystal (which has only $Q^2$ groups). A correlation was found between the shape of the $Q^n$ distribution and the nucleation tendency of these glasses, indicating that similarities between the tetrahedra connectivities in glass and isochemical crystal has a role in determining the internal nucleation tendency of the metasilicate glasses studied. 

## 1. Introduction

One of the authors of this study [1] previously proposed that there are two classes of stoichiometric glass-forming systems: for the first, the volume (presumed to be homogeneous) nucleation rates are experimentally detectable and the temperatures of maximum nucleation rate are the *same* or *greater* than the glass transition temperature ($T_g$). For typical laboratory conditions, i.e., using centimeter size samples that are heat-treated for a few hours above $T_g$, the second class of glasses only crystallize heterogeneously by surface nucleation or aided by nucleating agents. For this second family of glasses, the expected temperatures of maximum homogeneous nucleation rates (calculated by the classical nucleation theory) are less than $T_g$. Thus, it is possible to classify the crystal nucleating ability of different systems by this criterion.

There are a number of questions concerning the crystal nucleation kinetics in glasses. One of the

* Corresponding author. Tel.: +55-16 273 9755; fax: +55-16 271 3616.
*E-mail address:* valmor@if.sc.usp.br (V.R. Mastelaro).

0022-3093/00/$ - see front matter 
PII: S0022-3093(00)00139-3

proposed hypotheses postulates that the nucleating tendency depends on the structural similarity between the parent glass and its isochemical crystal phase [2–7].

In qualitative terms, the degree of structural similarity between parent glass and resulting crystal should affect the main thermodynamic parameters controlling nucleation; liquid-crystal surface energy ($\sigma$) and thermodynamic driving force ($\Delta G$), thus affecting the nucleation ability of the system. The homogeneous nucleation rate is given by: $I \sim (K'/\eta)\exp(-K''\sigma^3/T\Delta G^2)$, where $K'$, $K''$ are constants, $\eta$ is the viscosity and $T$ is the temperature. Hence, the surface energy dominates due to its power-3 against power-2 for $\Delta G$. The exact relationships of the structural parameters of glass and crystal with surface energy and driving force are not known; however, there should be some optimum structural similarity. This idea is clarified if we analyze two limiting cases: (i) when the structures of glass and isochemical crystal are too different, then $\sigma$ should be too large, inhibiting nucleation. On the other hand, in the hypothetical case, (ii) when the structures of glass and crystal are almost identical, $\sigma$ should vanish (which would enhance nucleation), however, $\Delta G$ should also tend to zero, precluding nucleation.

To further test this hypotheses, in this article we measure and compare the local structures of the network-forming cation $Si^{4+}$ ($Q^n$ groups) in four metasilicate glasses that have different volume nucleation rates, i.e.: $Na_2Ca_2Si_3O_9$ and $Na_4CaSi_3O_9$ (largest), $CaSiO_3$ (intermediate) and $CaMgSi_2O_6$ (undetectable nucleation rates).

## 2. Literature review

We will sum up here some of the most relevant studies that propose the existence of a structural relationship between the parent glass and its isochemical crystal and the nucleating ability of the glass.

In 1984, Schramm et al. [3] analyzed the devitrification of lithium silicate glasses using $^{29}Si$ magic angle spinning nuclear magnetic resonance (MAS–NMR). Their studies concentrated on glassy and crystalline $Li_2O$–$2SiO_2$ (LS2). They found that the most abundant species in LS2 glass are the $Q^3$ species (3 is the number of bridging oxygen per $SiO_4$ tetrahedra). In fact, they obtained the following distribution of $Q^n$ species: 22% $Q^2$, 57% $Q^3$, 14.6% $Q^4$ and 6.4% $Q^0 + Q^1$. As the LS2 crystal should have 100% $Q^3$, the authors mentioned that the glass had a sufficiently large concentration of $Q^3$ units to induce crystallization. Moreover, the mean chemical shift of $Q^3$ (−92 ppm) in the glass was similar to that observed in its crystalline phase (−93 ppm). Based on the correspondence of the chemical shifts, they suggested that the local silicon environments in both phases are similar and concluded that glasses of the $Li_2O$–$SiO_2$ system easily nucleate (which, in fact, they do) because the local environment of silicon in the glass is compatible with those in the isochemical crystal. We will show later that this relationship between the chemical shifts of glasses and crystals that easily nucleate does not hold true for a number of systems.

Dickinson [4] compared the structure of glassy and crystalline $K_2TiSi_3O_9$ and analyzed the hypothesis that structural similarity/dissimilarity between the amorphous and crystalline phases could affect nucleation. Heat treatments of glassy $K_2TiSi_3O_9$ showed that only surface crystallization took place. Using Raman spectroscopy and extended X-ray absorption fine structure (EXAFS), he observed that there is a clear difference in the local structures of crystalline and glassy $K_2TiSi_3O_9$. Whereas the short-range structure of the crystal is typical of metasilicates, with the intermediate range order of ring silicates, the structure of the glass does not have this type of local and intermediate range structure. Instead, the glass contains more polymerized species (three bridging oxygens, BO), in addition to species with two BO. Furthermore, he observed that the largest difference is in the Ti coordination, for which there is a change in coordination from the regular octahedron of the crystal to mixed 5- and 6-coordination in the glass. Dickinson [4] attributed this large difference in the structures of the crystalline and glassy phases to the fact that this glass has an undetectably small volume nucleation rate.

Looking at it from a more macroscopic structural perspective, Zanotto and Muller [5] proposed

a simple method to predict the nucleation tendency in glass. Their approach was based on the following argument: if the structures of both glass and isochemical crystal phases are similar for compositions that nucleate homogeneously, then the mass densities, $\rho$, of glass and crystal must be similar. On the other hand, large differences between the densities of glass and crystal should be expected for compositions that nucleate heterogeneously. After analyzing the densities of isochemical glassy and crystalline phases for various stoichiometric systems belonging to both families, they concluded that if the density difference between a glass and its crystalline phase is significant (>10%), it will most likely only nucleate heterogeneously. On the other hand, if the densities are comparable, homogeneous crystal nucleation could occur. In fact, they found some exceptions to this rule because some glasses that only nucleate heterogeneously also have similar densities in the crystal phase. They ascribed these exceptions to the fact that comparable densities do not imply similar structures for glass and crystal, but that the opposite is true, i.e., different densities denote distinct structures. Thus, they concluded that similar densities for glass and isochemical crystal is a *necessary but not sufficient* condition for structural similarity and, inferentially for homogeneous nucleation.

Using the classification proposed in Ref. [5], for the metasilicate glasses considered in this study we find that glassy and crystalline $Na_2Ca_2Si_3O_9$, $Na_4CaSi_3O_9$ and $CaSiO_3$ have density differences $(\Delta\rho/\rho_{glass})$ of 1.8%, 3.8%, and 6.6%, respectively, while this difference is 18.5% for $CaMgSi_2O_6$. Indeed, volume nucleation is easily detected in the first three systems, while the last only has surface nucleation on laboratory scale. However, as comparable densities for glass and crystal do not unequivocally imply similar structures, it would be interesting to obtain quantitative structural data for the above systems. We will show later that the local structures of the network *modifier* cation, Ca, have been determined in two of these systems. Hence, in this work, we extend the structural analysis to the network-*forming* atoms, Si, for these systems.

Muller et al. [6] tested the hypotheses that structural similarity at a molecular level between glass and crystal should favor volume nucleation. Literature data for the molecular structures of several silicate glasses that nucleate homogeneously and heterogeneously were critically analyzed. A comparison was made with the structures of their equilibrium crystalline phases. Muller et al. did, in fact, observe that for glasses in which homogeneous nucleation occurs, the structural arrangements in glass and isochemical crystal appear to be similar while for glasses displaying heterogeneous nucleation, the local structures of glass and crystal is different. In short, they concluded that it is possible to predict the nucleation tendency by comparing the molecular structure of the glass and the phase crystallized from such glass. However, we emphasize that only available literature data resulting from a number of different studies and often employing different structural techniques, were used in the study of Muller et al. [6].

Recently, aiming at more systematic results regarding the short range structure around the network *modifiers* in glasses and crystals, Mastelaro et al. [7] undertook an EXAFS analysis of calcium and lead in three different silicate glasses: $CaSiO_3$ and $Na_2Ca_2Si_3O_9$ (for which volume nucleation is observed) and $PbSiO_3$ (for which nucleation only occurs on samples surfaces). The results indicated that, for the two glasses that nucleate internally, the local structure of Ca was similar to its short-range order in the corresponding crystalline phases. On the other hand, the short-range order of the glass that only nucleates heterogeneously differed from that of its isochemical crystal. Hence, the proposed relationship between the local structure and the nucleation mechanism was corroborated by the EXAFS analysis.

As demonstrated in the summary of previous research, there is growing evidence to support the hypotheses that glasses that have detectable homogeneous nucleation rates have local structures similar to the crystalline phases formed in them, and vice versa. However, quantitative structural information using the *same* experimental technique for glasses and isochemical crystals (synthesized by devitrification), for both classes of systems, were only obtained for the network

modifiers. Therefore, the purpose of this work is to make a quantitative analysis of the short-range structure around the network-forming cation $Si^{4+}$ ($Q^n$ groups). With this information, we hope to verify the possible relationship of these groups in glass and corresponding crystal with the nucleation tendency. Four stoichiometric metasilicate glasses having different volume nucleation rates are considered. Quantitative $^{29}Si$ MAS–NMR spectra were obtained for these glasses and their corresponding crystalline phases obtained by devitrification.

## 3. Experimental

The glasses were prepared by melting homogeneous mixtures of analytical grade reagents in 100-ml Pt crucibles, in electric furnaces. The melting temperatures ranged from 1450°C to 1550°C, with a hold time of about 2 h. The liquids were then cast between cold steel plates and manually pressed at an estimated cooling rate between 100°C/s and 500°C/s. To obtain fully crystallized samples, the specimens were subjected to nucleation and development treatments, which were chosen after a differential scanning calorimetry (DSC) analysis. The $Na_2Ca_2Si_3O_9$ glass sample was heated at 600°C for 24 h and then at 690°C for 20 min; the $Na_4CaSi_3O_9$ glass sample was heated at 505°C for 12 h and then at 596°C for 8 h; the $CaSiO_3$ glass sample was heated at 725°C for 120 h and then at 885°C for 12 h and, finally, the $CaMgSi_2O_6$ glass sample was heated at 874°C for 22 h and then at 877°C for 25 h. The four metasilicate glasses measured in this work have different internal nucleation rates: $Na_4CaSi_3O_9$ ($I_{max} \approx 10^{14}$ $m^{-3}$ $s^{-1}$), $Na_2Ca_2Si_3O_9$ ($\approx 10^{12}$ $m^{-3}$ $s^{-1}$), $CaSiO_3$ ($\approx 10^{6}$ $m^{-3}$ $s^{-1}$) and $CaMgSi_2O_6$ ($< 10^{3}$ $m^{-3}$ $s^{-1}$) [1].

The crystalline phases obtained through devitrification were measured by X-ray diffraction (XRD). Diffractograms were obtained in an automatic difractometer (Rigaku Rotaflex model RU200B), with nickel filtered CuK$\alpha$ radiation (1.540 Å). Figs. 1 and 2 present the XRD patterns of the $Na_2Ca_2Si_3O_9$ and $Na_4CaSi_3O_9$ (Figs. 1(a) and (b)) and $CaSiO_3$ and $CaMgSi_2O_6$ (Figs. 2(a) and (b)).

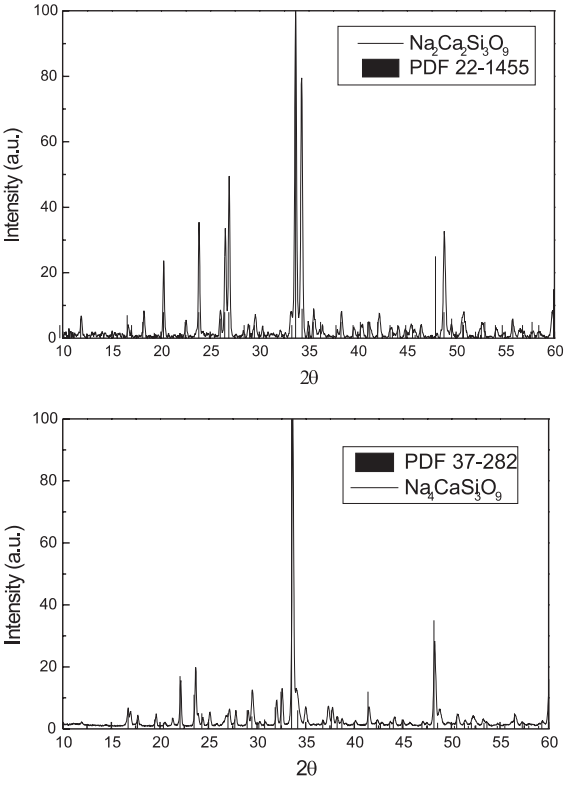


Fig. 1. XRD patterns of $Na_2Ca_2Si_3O_9$ and $Na_4CaSi_3O_9$ crystalline phases.

High resolution $^{29}Si$–NMR spectra were obtained in magnetic field of 9.4 T, at a frequency of 79.45 MHz, with a spectrometer (Varian Unity INOVA). Measurements were carried out under magic-angle sample spinning (MAS) of up to 5 kHz, using a 7 mm wide-body CP/MAS probe (from Varian) and 7 mm zirconia rotors. The spectra were obtained from Bloch decay (BD) signals after $\pi/2$ pulses of 4 μs length. Relatively long recycle times were used to avoid any possible effects of differential relaxation across the inhomogeneously broadened NMR line. No saturation of the NMR signal was detected using recycle times exceeding 250 s. Up to 600 free induction decay (FID) signals were collected and averaged. The resonance line of a polycrystalline kaolinite sample was used as the secondary external standard for referencing chemical shifts (−91.2 ppm in respect to tetrametilsilane, TMS).

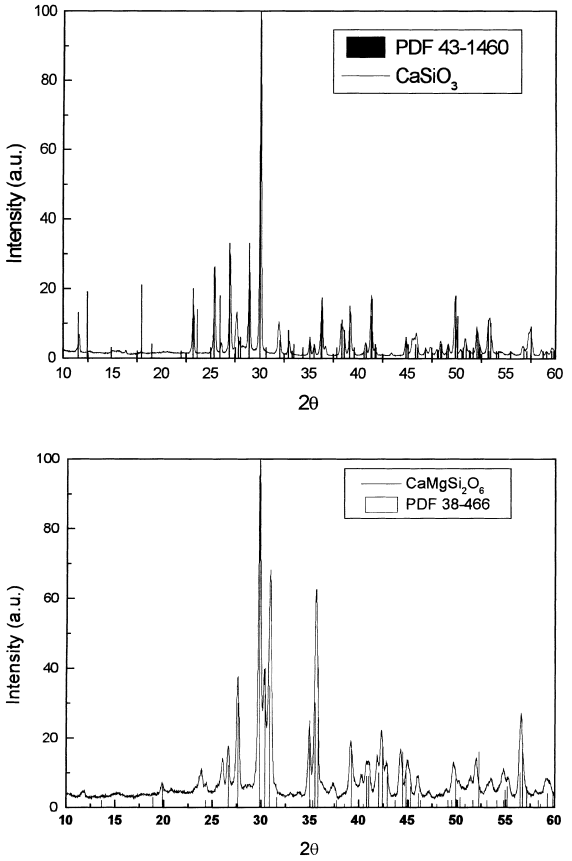


Fig. 2. XRD patterns of $CaSiO_3$ and $CaMgSi_2O_6$ phases.

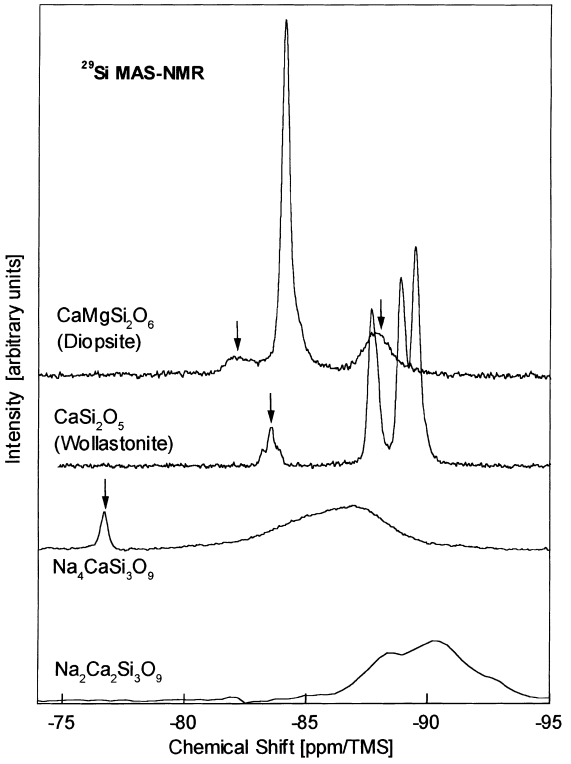


Fig. 3. High resolution $^{29}$Si–NMR spectra of crystalline samples. Arrows points to resonance lines associated with impurity phases present in the specimens (see text for details).

## 4. Experimental results

The XRD patterns presented in Figs. 1 and 2 were indexed according to the JCPDS powder diffraction files [8–11]. However, one or two crystallographic peaks in the XRD could not be indexed, indicating that the solids obtained after the crystallization could contain minor quantities of other crystalline phases. We used the crystalline compounds as a reference for the interpretation of the NMR spectra of the glasses.

Fig. 3 shows the high-resolution $^{29}$Si–NMR spectra of the four crystalline samples. A number of resonance lines can be observed, with a full with at half maximum (FWHM) typically less than 2 ppm. Table 1 shows the results for the isotropic chemical shift and the integrated intensity of each line, obtained from a multiple lorentzian fitting to the experimental data. The attribution of NMR lines to $Q^n$ groups was done by considering the stoichiometry and crystallographic data of each material. Fig. 4 shows the $^{29}$Si–NMR spectra of the corresponding samples. For each glass, a resonance line covers the chemical shift range of silicon in several $Q^n$ groups with $n = 0, \ldots, 4$. A deconvolution of the spectra was performed to obtain the $Q^n$ distribution, using the common assumption of Gaussian distributions of isotropic chemical shifts for each type of $Q^n$ unit [12–14]. Unfortunately, overlapping of $Q^n$ resonances frequently occur, giving co-variances between best-fit intensity parameters and, consequently, to uncertainties regarding the relative populations of the $Q^n$ species. To minimize these problems, some physical criteria were imposed on the fitting procedure to discard unrealistic numerical results. Thus, FWHMs of individual Gaussians were re-

Table 1
Isotropic chemical shifts and line intensities of the $^{29}$Si–NMR lines of the crystalline samples (possible identification of minor phases are discussed in the text)

| Crystal | | Center (ppm) | Area (%) |
|---|---|---|---|
| $Na_2Ca_2Si_3O_9$ | $Q^2$ | $-88.2 \pm 0.3$ | –[a] |
| | | $-90.4 \pm 0.3$ | –[a] |
| | | $-92.8 \pm 0.3$ | –[a] |
| | $Q^2$ [b] | $-76.7 \pm 0.2$ | $7 \pm 1$ |
| $Na_4CaSi_3O_9$ | $Q^2$ | $-85.0 \pm 0.3$ | –[a] |
| | | $-87.0 \pm 0.3$ | –[a] |
| | $Q^2$ [c] | $-83.5 \pm 0.4$ | $8 \pm 1$ |
| Wollastonite | $Q^2$ | $-87.8 \pm 0.2$ | $28 \pm 5$ |
| | | $-88.9 \pm 0.2$ | $29 \pm 5$ |
| | | $-89.5 \pm 0.2$ | $35 \pm 5$ |
| | $Q^2$ [d] | $-82.0 \pm 0.5$ | $5 \pm 2$ |
| Diopside | $Q^2$ | $-84.0 \pm 0.2$ | $77 \pm 4$ |
| | $Q^2$ [e] | $-88.0 \pm 0.5$ | $18 \pm 3$ |

[a] Strongly overlapped.
[b] Impurity phase, possibly $Na_2SiO_3$.
[c] Impurity phase, pseudo wollastonite.
[d] Impurity phase, orto-ensteatite.
[e] Impurity phase, wollastonite.

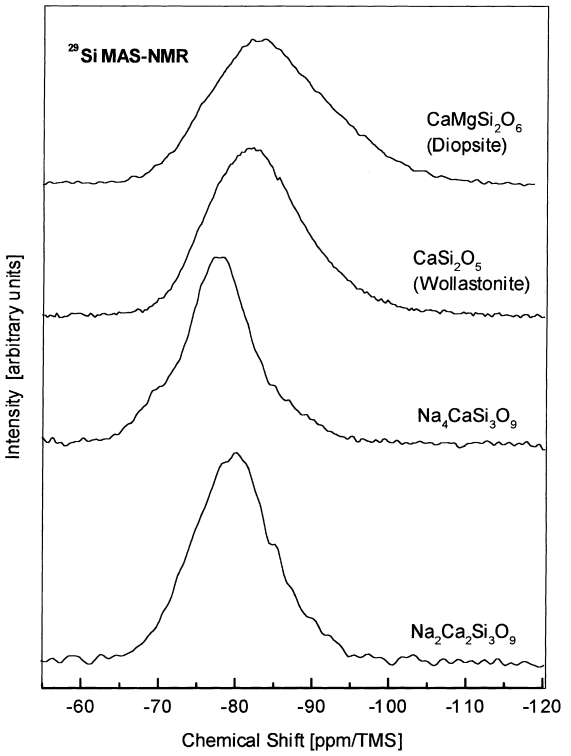


Fig. 4. High resolution $^{29}$Si–NMR spectra of glassy samples.

stricted to less than 20 ppm, based on the chemical shifts observed in different crystalline silicates [15]. In addition, the centers of adjacent Gaussians from different $Q^n$ units had to be separated by more than 5 ppm. The number of Gaussians used in each case was determined by the chemical shift range spanned by the NMR spectrum and other spectral features, such as partially resolved bumps or asymmetries. With these criteria, up to four partially overlapped Gaussian distributions were needed to deconvolute these spectra. Equivalent acceptable fittings were obtained from deconvolutions with three and four Gaussian functions. To choose the physically significant fittings, stoichiometric criteria and literature data of chemical shifts were considered.

For glassy wollastonite and diopside, though small, there is an appreciable spectral intensity in the chemical shift range of $Q^4$ ($-115$ to $-100$ ppm), which is rarely overlapped with $Q^3$ [15]. It is, therefore, possible to ensure the existence of $Q^4$ groups in these glasses. Conversely, the NMR spectra of glassy $Na_2Ca_2Si_3O_9$ and $Na_4CaSi_3O_9$ samples indicate that there are *no* $Q^4$ groups in their networks. Additionally, the identification of $Q^2$ resonances was done assuming that the distribution of $Q^n$ species in metasilicates must satisfy the stoichiometric condition $Q^0 + Q^1 = Q^3 + Q^4$, so that the average is always $Q^2$. Thus, the remaining resonances were readily assigned.

Table 2 shows the fitted parameters for the chemical shift distributions of each $Q^n$ group in the four samples. For wollastonite and diopside, four Gaussian deconvolutions were performed because of the presence of $Q^4$ groups, while for $Na_2Ca_2Si_3O_9$ and $Na_4CaSi_3O_9$ samples, only three Gaussian functions were used. If a fourth Gaussian is added, its chemical shift cannot be assigned to $Q^0$ or $Q^4$ species. Separations of approximately 7 ppm between the centers of $Q^n$ and $Q^{n+1}$ distributions were obtained in all glasses, with FWHM varying from 7 to 12 ppm. Although the $Q^0 + Q^1 = Q^3 + Q^4$ constraint was not imposed in the fittings, Table 2 shows that this condition was

Table 2
Chemical shifts, line-widths and integrated intensities of the $^{29}$Si–NMR lines corresponding to different $Q^n$ units in the four glasses[a]

| Composition | | Crystal $\delta$ (ppm) | Glass | | | Chemical shift difference for $Q^2$ in crystal – glass δ-center (ppm) |
|---|---|---|---|---|---|---|
| | | | Center (ppm) ±0.5 ppm | FWHM[b] (ppm) ±1 ppm | Area (%) | |
| $Na_2Ca_2Si_3O_9$ | $Q^1$ | | −73.4 | 9 | 16 ± 5 | |
| | $Q^2$ | −88.2/−90.4/−92.8 | −80.0 | 10 | 72 ± 8 | 8.2/10.4/12.8 |
| | $Q^3$ | | −88.5 | 9 | 12 ± 5 | |
| $Na_4CaSi_3O_9$ | $Q^1$ | | −70.0 | 7 | 14 ± 5 | |
| | $Q^2$ | −85/−87 | −77.5 | 8 | 67 ± 8 | 7.5/9.5 |
| | $Q^3$ | | −85.3 | 9 | 19 ± 7 | |
| Wollastonite | $Q^1$ | | −75.6 | 10 | 20 ± 5 | |
| | $Q^2$ | −87.8/−88.9/−89.5 | −82.6 | 11 | 64 ± 8 | 5.2/6.3/6.9 |
| | $Q^3$ | | −91.8 | 11 | 14 ± 5 | |
| | $Q^4$ | | −103.3 | 11 | 2 ± 1 | |
| Diopside | $Q^1$ | | −77.5 | 11 | 28 ± 8 | |
| | $Q^2$ | −84 | −84.0 | 11 | 43 ± 10 | 0 |
| | $Q^3$ | | −92.7 | 12 | 25 ± 6 | |
| | $Q^4$ | | −103.0 | 12 | 4 ± 1 | |

[a] For comparison, the values of isotropic chemical shift $\delta$ for the main resonance lines in crystals and their difference respect to the $Q^2$ central chemical shift in glasses are also shown.
[b] FWHM: full width at half maximum.

met for all samples, within the uncertainty of the numerical procedures. For clarity, we will describe and compare the results for each glass and crystal separately.

### 4.1. $CaSiO_3$ (wollastonite)

This glass has a small volume nucleation rate. At room temperature, the stable crystalline forms of $CaSiO_3$ contain 'dreier' single chains of silicate tetrahedra [16–18]. Thus, there are three different $Q^2$ sites for silicon in the unit cell. The $^{29}$Si–NMR spectrum of the crystalline wollastonite does, indeed, show three resolved resonance lines at −89.5, −88.9 and −87.8 ppm associated with these sites, with 93% of the total integrated intensity observed. These chemical shifts agree with previous observations of Smith et al. [19] and Mägi et al. [20], who detected a broader line centered at around −89 ppm. The remaining 7% of the silicon contributing to the NMR spectrum corresponds to a smaller resonance line at −83.5 ppm. Its isotropic chemical shift seems rather shielded to correspond to $Q^1$ chain terminators generated by absent tetrahedra. Furthermore, the existence of a number of non-bridging O–H groups can be disregarded since no $^{29}$Si–NMR signal was detected after $^1$H–$^{29}$Si cross-polarization experiments performed on this sample. Based on the chemical shift, 4 ppm less shielded than the main resonance lines, we might suggest Al substitution for Si, giving rise to a $Q^2$(1 Al) silicon resonance. Nevertheless, this substitution is an unlikely possibility because no $^{27}$Al–NMR signal was obtained from Bloch decay experiments, even after considerable signal averaging. Then, the −83.5 ppm resonance probably originates from a small fraction of another of the known forms of wollastonite, differing in the arrangement of the silicate chains. In fact, Mägi et al., reported for pseudo-wollastonite a resonance line exactly at −83.5 ppm [20].

The following distribution was obtained from the deconvolution of the NMR spectrum of the glassy wollastonite sample: 20% $Q^1$, 64% $Q^2$, 14%

$Q^3$ and 2% $Q^4$. Thus, the largest amount of silicon in glass and crystal samples corresponds to $Q^2$ groups. It is useful to compare these fractions with those obtained by Zhang et al. [12,14]. They applied a 2D $^{29}$Si–NMR technique to correlate isotropic (MAS) and anisotropic (off-MAS) spectra of glassy wollastonite. They obtained more accurate percentages for the $Q^n$ distribution with respect to the usual method of fitting the 1D MAS spectrum. They obtained $Q^0 = 0.7 \pm 0.1\%$, $Q^1 = 19.3 \pm 0.3\%$, $Q^2 = 54.7 \pm 0.3$, $Q^3 = 24.1 \pm 0.5\%$ and $Q^4 = 1.1 \pm 0.1\%$, which are comparable with our results (the difference for the most abundant species, $Q^2$, is about 15%). Considering that the 2D approach should be more precise, we assume that the $Q^n$ determination method used in this work presents a maximum discrepancy of 15%, based on the difference for the $Q^2$ fraction. As for the center of chemical shift distributions, the ones shown in Table 2 compare with those reported by Zhang et al. [14]: −74.6 ppm for $Q^1$, −81.7 ppm for $Q^2$ and −90.4 ppm for $Q^3$.

### 4.2. $CaMgSi_2O_6$ (Diopside)

This sample has an undetectable homogeneous nucleation rate. Crystallographic data of diopside indicates that the silicate tetrahedra are arranged in 'infinite' linear chains, with only one non-equivalent silicon site in the unit cell [21]. Fig. 3 actually shows that the NMR spectrum of the crystal has three resonance lines. The most intense line (77%), centered at −84 ppm with 0.5 ppm FWHM, corresponds to $Q^2$ units. Two other smaller and broader lines are observed at −88 ppm (18%) and −82 ppm (5%), which are also in the $Q^2$ chemical shift range. Previous NMR measurements made by Smith et al. [19] and Mägi et al. [20] have shown a single resonance centered at −85 ppm, a shift comparable to that obtained in our measurement for the strongest resonance, but with 5 ppm FWHM. $^{27}$Al NMR experiments were also performed on our sample; however, no appreciable signal was detected, indicating that Al, if present, are in concentrations too small to be detected by NMR. On the other hand, effects of hydration as those observed by Peck et al. [22] can also be disregarded in this case, because no signal was observed after $^1$H–$^{29}$Si cross polarization experiments. Therefore, we associated the smaller NMR lines to sample inhomogeneities, possibly distorted wollastonite (−88 ppm line) and orthoenstatite, $Mg_2Si_2O_6$, (−82 ppm line), the last one according to the measurements reported in Ref. [20].

For the glassy sample, the distribution of $Q^n$ units was: 28% $Q^1$, 43% $Q^2$, 25% $Q^3$ and 4% $Q^4$. To the best of our knowledge, only one MAS–NMR experiment has so far been reported for diopside by Murdoch et al. [23]. No quantification of the $Q^n$ species was made. The maximum of the spectrum was located at −82.0 ppm and, by analogy with the observed chemical shift of $Q^2$ units in the crystal, Murdoch et al. concluded that the dominant connectivity in the network is $Q^2$. The deconvolution of our spectrum gives 43% $Q^2$ with a chemical shift at around −83.0 ppm. Therefore, our results agree with those reported in Ref. [23].

### 4.3. $Na_2Ca_2Si_3O_9$

As mentioned earlier, this glass has the largest homogeneous nucleation rate in the studied set of samples. In crystalline $Na_2Ca_2Si_3O_9$, the silicon is organized in six-membered rings with a $C_2$ symmetry [24]. Thus, there are three different Si sites with $Q^2$ connectivity in the unit cell. Accordingly, (Fig. 3) the NMR spectrum is composed of three partially resolved resonance lines centered at −88.2, −90.4 and −92.8 ppm. Due to the partially disordered structure of the $Na_2Ca_2Si_3O_9$ crystal, where Na/Ca sites with fractional occupation number were determined from XRD [24], the resonance lines are broader than those from wollastonite and diopside. For the glassy sample, the most satisfactory fitting gives the following distribution of species: 16% $Q^1$, 72% $Q^2$ and 12% $Q^3$. On the other hand, as seen in Table 2, resonance lines in the crystalline state appear more shielded with respect to the center and width of the fitted $Q^2$ distribution in the glass (−80.0 ppm).

### 4.4. $Na_4CaSi_3O_9$

This glass has a similarly large homogeneous nucleation rate. As far as we know, crystallographic data are not available for this material.

However, since it is a metasilicate, according to stoichiometric considerations only $Q^2$ groups should exist in the homogeneous crystal. As shown in Fig. 3, there are at least two overlapping lines in the NMR spectra, at approximately −85 and −87 ppm, which are associated with $Q^2$ species. The total width of the group of lines is 4 ppm, a width identical to that observed in the spectrum of crystalline $Na_2Ca_2Si_3O_9$. Thus, the presence of additional unresolved $^{29}Si$ lines cannot be disregarded in $Na_4CaSi_3O_9$. Also, occupational disorder in the crystalline structure may be responsible for the broadening of the resonance lines, as in $Na_2Ca_2Si_3O_9$. On the other hand, the NMR spectrum of this crystal has a resonance (0.35 ppm FWHM) centered at −76.7 ppm. In different crystal samples prepared from the same glass rod, this signal appeared with varying intensity (from 5% to 8%), without changes in the shape of the other lines. The smaller FWHM of this minor signal indicates that silicon atoms are located in a more ordered structure, as compared with those silicons contributing to the resonances at −85/−87 ppm. Based on this fact, we could assign the −76.7 ppm resonance to an impurity silicate phase, perhaps $Na_2SiO_3$, which has a single $Q^2$ resonance at −76.8 ppm [20]. For the glassy $Na_4CaSi_3O_9$ sample, the following distribution of $Q^n$ units resulted: 14% $Q^1$, 67% $Q^2$, 19% $Q^3$.

## 5. Discussion

As we have briefly described before, Schramm et al. [3] reasonably proposed that the LS2 glass (we emphasize that this composition is *not* a metasilicate) has a high tendency to homogeneous crystallization owing to:

(a) Local structural similarity between the glass and crystalline phases, inferred from the similarity of the chemical shifts for $Q^3$ in glassy and crystalline LS2.

(b) High concentration of $Q^3$ in the glass (greater than 50%).

In the set of metasilicate glasses studied in this work, only criterion (b) applies (for $Q^2$ instead of $Q^3$). The overall $Q^n$ distribution can be visualized in Fig. 5, where integrated intensities are plotted as a function of the central chemical shift for $Q^n$ resonance. $Na_2Ca_2Si_3O_9$, $Na_4CaSi_3O_9$ and wollastonite glasses have similar $Q^n$ distributions, $Q^2$ being the most abundant species (72%, 67% and 64–55%, respectively). From the overall shape of these distributions, we propose that the short-range order around $Si^{4+}$ in the glass is more similar in respect to its crystal phase (where only $Q^2$ connectivities exist) for the systems with sharper distributions.

Due to the presence of $Q^4$ units, wollastonite has a slightly wider distribution than Na-containing glasses. Diopside has a substantially smaller content of $Q^2$ species (43%) and, consequently, has the larger $Q^n$ distribution among the studied glasses. Therefore, glasses having the greatest nucleating ability have a considerable amount of tetrahedra having the same connectivity as in the crystal phase and a smaller width of the $Q^n$ distribution.

On the other hand, there are *significant differences* between the chemical shifts of the $Q^2$ species in the glasses and isochemical crystals. Resonance in crystalline $Na_2Ca_2Si_3O_9$, $Na_4CaSi_3O_9$ and wollastonite are systematically more shielded than the corresponding $Q^2$ resonance in glasses. Table 2 shows that the chemical shift differences are considerable and are even comparable to the FWHM of the $Q^n$ distributions in the glasses. Therefore,

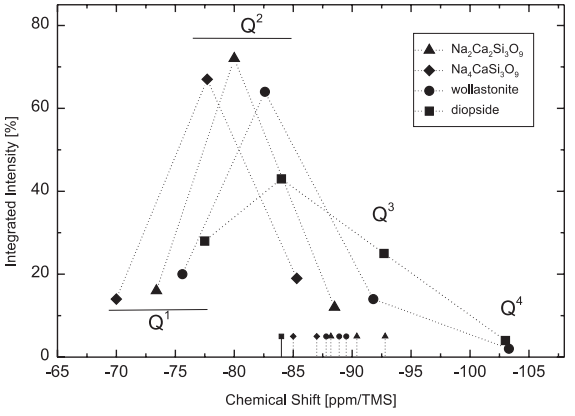


Fig. 5. Integrated intensities for the Gaussian $Q^n$ distributions of isotropic chemical shift for each glass. The chemical shifts correspond to the centers of the $Q^n$ distributions. The points with sticks in the lower part of the plot show the positions of the main $Q^2$ resonance lines observed in the corresponding isochemical crystals.

there are appreciable structural differences in the environment of $Q^2$-units in glass and in crystal, despite the similarity in the dominant connectivity ($Q^2$) of the network-forming cations, although it is difficult to determine the extent of these differences. A deshielding effect on the silicon resonance in glass can be produced by geometrical distortions, such as longer Si–O distances or more acute Si–O–Si angles, and by weaker bonds between the modifier cation and O atoms [15]. It should be noted that, even in crystalline $Na_2Ca_2Si_3O_9$, there is a 4.5 ppm difference between two non-equivalent silicon atoms in the same 6-membered ring, a difference comparable to some differences observed between crystal and glass. Quite surprisingly to us is that the chemical shifts for the $Q^2$ groupings in crystalline and glassy diopside are in close agreement. It is impossible, however, to infer structural similarity from this coincidence because agreement between chemical shifts is only a *necessary* condition for local similarity.

Therefore, similarity in the overall degree of connectivity of the forming cations in glass and crystal, inferred from the shape of the $Q^n$ distribution, seems to be more important to internal nucleation than a close structural similarity around the $Q^2$ silicon atoms, probed by the chemical shifts. It is interesting to note (Fig. 5 and Table 1) that the centers of $Q^n$ distributions in $Na_4CaSi_3O_9$ glass are systematically shifted by approximately 3 ppm in respect to the corresponding ones in $Na_2Ca_2Si_3O_9$ glass. The same shift is detected for the $Q^2$ species in the crystal: the group of lines are centered at around −90 ppm in $Na_2Ca_2Si_3O_9$ and at −87 ppm in $Na_4CaSi_3O_9$, spanning a 5 ppm range in the spectrum. Based on these results we suggest a similar structural relationship between the glass and the crystal phase for both compositions.

The silicon–oxygen tetrahedra in the crystalline phases are organized in $Q^2$ groups, forming rings (in $Na_2Ca_2Si_3O_9$ and possibly in $Na_4CaSi_3O_9$) or chains (in wollastonite and diopside). Though high-resolution 1D-NMR can probe the distribution of Si in terms of $Q^n$ units, it shows very little about the topological relationships among these groups. The local range of the 1D-NMR experiment, restricted to a typical radius of 1 nm, gives little information about tetrahedral neighbors outside the first coordination sphere. An exploration of medium range connectivities in glasses with extreme nucleation and qualitatively different $Q^n$ populations, such as those observed in $Na_2Ca_2Si_3O_9$ and diopside, would be very useful.

In summary, the systems that have the largest nucleation rates ($Na_2Ca_2Si_3O_9$ and $Na_4CaSi_3O_9$) have the largest percentage of $Q^2$ units (72% and 67%, respectively) and the smallest $Q^n$ distributions. The only other groupings in these glasses are $Q^1$ and $Q^3$. Wollastonite, having a lower nucleation rate than Na-containing glasses, has a smaller $Q^2$ content (64%), but some amount of $Q^4$ is detected in this glass, widening its $Q^n$ distribution. Diopside, displaying undetectable homogeneous nucleation, has an even larger $Q^n$ distribution. Only 43% of the network-forming cations are organized in $Q^2$ units and, consequently, a larger fraction of $Q^1$, $Q^3$ and $Q^4$ species are present in this glass than in the other compositions.

Finally, we stress that while the correlation of the $Q^n$ distribution and nucleation tendency in the *metasilicate* glasses studied here is interesting, the possibility of a fortuitous coincidence should not be dismissed. Literature data for other systems, for instance, *disilicates* $Li_2O \cdot 2SiO_2$ (LS2), $Na_2O \cdot 2SiO_2$ (NS2), $K_2O \cdot 2SiO_2$ (KS2), show an opposite trend. In the case of these disilicates, for which the crystal phases are 100% $Q^3$, the crystal nucleation rates decrease from LS2 to KS2 while the amount of $Q^3$ increase in that order: 63–71% $Q^3$ in LS2, 79% $Q^3$ in NS2 and 86% $Q^3$ in KS2 [25]. These findings deserve further attention. We hope that the present study encourages similar analyses of a broader set of metasilicate glasses, in order to check whether there is or not a general trend for metasilicates.

## 6. Conclusions

The differences in the chemical shifts of the predominant $Q^2$ species in glass and crystal indicate short range differences between the silicon environments, even in those systems displaying the greatest nucleating ability. On the other hand, the

*shape* of the $Q^n$ distribution, indicating the degree of similarity between silicate connectivity in glass and isochemical crystal, shows a correlation with the internal nucleation tendency of the four metasilicate glasses studied.

We should stress, however, that while the correlation of the $Q^n$ distribution and nucleation tendency in the metasilicate glasses studied here is quite interesting, the possibility of a fortuitous coincidence cannot be dismissed. Literature data for other families of glasses, for instance, disilicates, do not show the same trend. Thus, to generalize the present findings for metasilicates, and to seek plausible explanations for the phenomenon, additional effort should be directed to verify the existence of the correlation in other metasilicate systems.

## Acknowledgements

J.S. thanks FAPESP (Fundação de Amparo à Pesquisa do Estado de São Paulo, Brazil) for a post-doctoral fellowship. The critical comments of Boris A. Shakmatkin and Natalia M. Vedishcheva from the Institute of Silicate Chemistry, St. Petersburg, are fully appreciated. Funding by CNPq, PRONEX and FAPESP (grant no. 99/0871-2) is deeply appreciated.

## References

[1] E.D. Zanotto, J. Non-Cryst. Solids 89 (1987) 361.
[2] B.H.W.S. de Jong, W.S. Keefer, G.E. Brown, Ch.M. Taylor, Geochim. Cosmochim. Acta 45 (1981) 1291.
[3] C.M. Schramm, B.H.W.S. de Jong, V.E. Parziale, J. Am. Chem. Soc. 106 (1984) 4396.
[4] J.E. Dickinson, in: Proceedings of the XV International Congress on Glass, Leningrad, vol. 1a, 1989, p. 192.
[5] E.D. Zanotto, E. Muller, J. Non-Cryst. Solids 130 (1991) 220.
[6] E. Muller, K. Heide, E.D. Zanotto, J. Non-Cryst. Solids 155 (1993) 56.
[7] V.R. Mastelaro, E.D. Zanotto, N. Lequeux, R. Cortés, J. Non-Cryst. Solids 262 (2000) 191.
[8] Powder Diffraction File No. 22-1455, JCPDS-ICDD 1983.
[9] Powder Diffraction File No. 12-670, JCPDS-ICDD 1983.
[10] Powder Diffraction File No. 11-654, JCPDS-ICDD 1983.
[11] Powder Diffraction File No. 27-88, JCPDS-ICDD 1983.
[12] P. Zhang, C. Dunlap, P. Florian, P.J. Grandinetti, I. Farnan, J.F. Stebbins, J. Non-Cryst. Solids 204 (1996) 294.
[13] J. Mahler, A. Sebald, Solid State Nucl. Magn. Res. 5 (1995) 63.
[14] P. Zhang, P. Grandinetti, J.F. Stebbins, J. Phys. Chem. B 101 (1997) 4004.
[15] G. Engelhardt, D. Michel, High Resolution Solid-State NMR of Silicates and Zeolites, Wiley, Norwich, 1987.
[16] Y. Ohashi, L. Finger, Carnegie Institution of Washington: Yearbook (CIWYA 75), 1976, p. 746.
[17] K.F. Hesse, Zeit. Krist. 168 (1984) 93.
[18] K. Mamedov, N. Belov, Dokl. Akad. Nauk SSSR 107 (1956) 463.
[19] K.A. Smith, R.J. Kirkpatrick, E. Oldefield, D.M. Henderson, Am. Mineral. 68 (1983) 1206.
[20] M. Mägi, E. Lipmaa, A. Samoson, G. Engelhardt, A. Grimmer, J. Phys. Chem. 88 (1984) 1518.
[21] B. Warren, W.L. Bragg, Z. Kristallogr. Kristall. Kristallphys. Kristallchem. 69 (1928) 168.
[22] J.A. Peck, I. Farnan, J.F. Stebbins, Geochim. Cosmochim. Acta 52 (1988) 3017.
[23] J.B. Murdoch, J.F. Stebbins, I.S.E. Carmichael, Am. Mineralogist 70 (1985) 332.
[24] H. Ohsato, Y. Takeuchi, I. Maki, Acta Crystallogr. C 42 (1986) 934.
[25] H. Maekawa, T. Maekawa, K. Kawamura, T. Yokokawa, J. Non-Cryst. Solids 127 (1991) 53.